

Supplementary Information for

Failure mechanism of 2D silicon film anodes: in-situ observations and simulations on crack evolution

1 Experimental

1.1 Electrochemical cell

Quartz wafers (500 μ m thick, double-side polished) were used as substrates for electrode fabrications. The current collectors and electrodes were deposited in a commercial magnetron sputtering system (Kurt J. Lesker LAB 18). First, the substrate was plasma-cleaned in Ar at 10 mTorr and RF power of 50W for 3min. Next, a 30nm Ti layer was sputtered on the Quartz wafer followed by deposition of ~300nm thick Cu layer as current collector. Then another 30nm Ti and ~300nm thick silicon layer were deposited. During deposition, the chamber pressure was kept at 3mTorr, and the RF power was 130w. Finally, the silicon thickness reached 311nm, which was measured by step profiler after deposition (figure S1). The home-made in-situ electrochemical cell (detail in figure S2 and S3) was assembled in a high-purity argon filled glove box (Mbraun Inc.) with H₂O and O₂ contents <10 ppm. The electrolyte consisted of 1 M LiPF₆ in 1:1 (v/v) DMC: EC.

1.2 In-situ & ex-situ optical characterization

An optical microscopy (Keyence Corporation) was used to in-situ characterize the continuous morphological changes of silicon films. The

morphological changes were also ex-situ imaged by a field-emission scanning electron microscopy (SEM, FEI Quanta 250). All electrochemical experiments were conducted using a charge/discharge battery testing system (Arbin Instruments) with a lithium foil counter electrode. The galvanostatic current density was $60 \mu\text{Acm}^{-2}$ and $30 \mu\text{Acm}^{-2}$ for discharge and charge, the cycled voltage range was run from 1.5V to 0.01V (vs. Li/Li⁺).

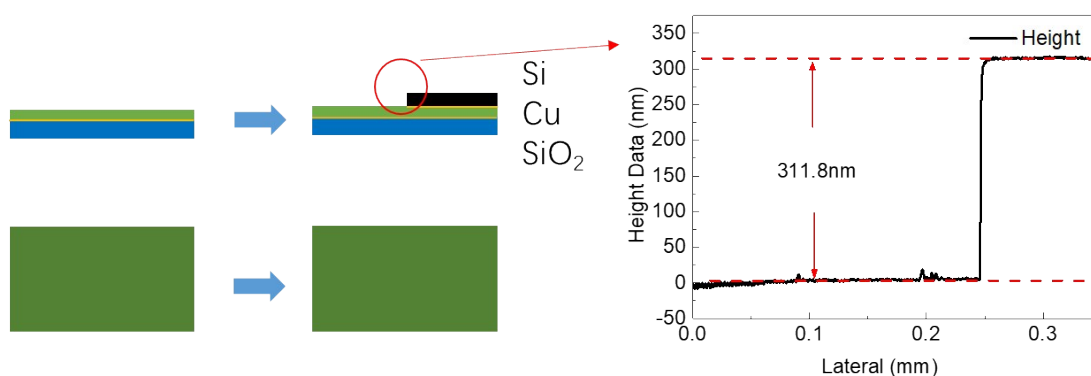


Figure S1. Schematic of the test electrode, and the result of the silicon thickness measured by step profiler.

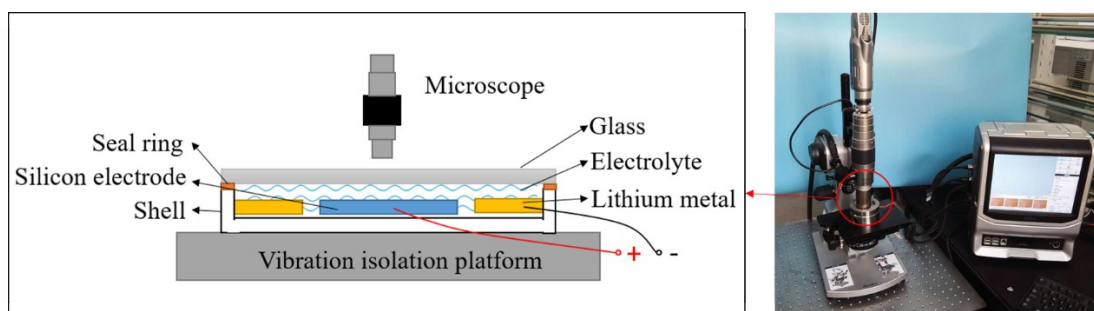


Figure S2. Schematic and the **photograph** of the in-situ optical system.

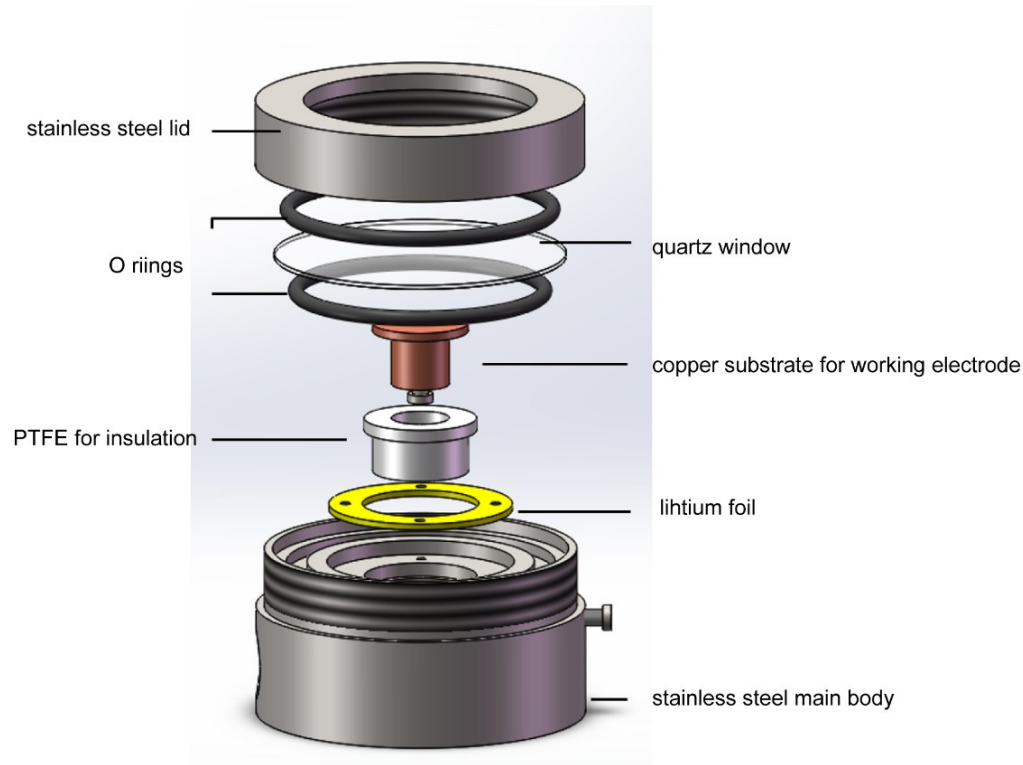


Figure S3. 3D structure of the in-situ electrochemical cell.

2 Finite element analysis (FEA) model

Substituting equation (4) into equation (3) The chemical potential per mole is given as

$$\mu = RT \ln \frac{\bar{C}}{1-\bar{C}} - \lambda_1 \lambda_2 \lambda_3 \sigma_h \frac{3}{\lambda^c} \frac{d\lambda^c}{dC} \quad \backslash * \text{MERGEFORMAT}$$

(S1)

The first term is the driving force for Li diffusion relates to the concentration gradient, and the third term shows the influence of stress on the chemical potential.

The mass flux of Li into silicon is also given in nominal quantities as

$$J_k = -\frac{CD}{RT} \frac{\partial \mu}{\partial X_k} \quad \backslash * \text{MERGEFORMAT (S2)}$$

where C is the nominal Li concentration, D is the diffusivity of in Li-Si

alloy.

The governing equations for the coupled large deformation and mass diffusion include mechanical equilibrium and mass conservation law as

$$\begin{aligned} \frac{\partial \sigma_{ij}}{\partial x_i} &= 0 \\ \frac{\partial C}{\partial t} + \frac{\partial J_K}{\partial X_K} &= 0 \end{aligned} \quad \backslash * \text{ MERGEFORMAT (S3)}$$

The mechanical equilibrium is written in terms of true stress σ_{ij} and current coordinates x_i at the current time t . The mass conservation law is expressed in the reference coordinates X_K at time t .

A dimensionless formulation is used. The energy per mole is normalized by RT (unit: J mole⁻¹); mole density is normalized by C_{max} (unit: mole m⁻³); length is normalized by a characteristic length H in the problem considered; and time is normalized by H^2/D . Thus, the following dimensionless quantities are defined: Li concentration $\bar{C} = C / C_{max}$, time $\tau = Dt/H^2$, coordinates $\bar{X}_K = X_K / H$, $\bar{x}_j = x_j / H$, chemical potential $\bar{\mu} = \mu / RT$, flux $J = J(L / C_{max} D)$, mobility tensor.

Based on the dimensionless parameters, the mass conservation law becomes

$$\frac{\partial \bar{C}}{\partial \tau} + \frac{\partial \bar{J}_k}{\partial \bar{X}_K} = 0. \quad \backslash * \text{ MERGEFORMAT (S4)}$$

The governing equation for heat transfer in ABAQUS is

$$\rho \frac{dU}{dT} \frac{\partial T}{\partial t} + \frac{\partial f_i}{\partial x_i} = r \quad \backslash * \text{ MERGEFORMAT (S5)}$$

where ρ is the density, U is the heat energy, T is the temperature, t is the

time, f_i is the true heat flux and r is the heat source. Rather than Eulerian description, it is an updated Lagrangian description which uses the converged coordinates from the last time step as the new reference state. The mass conservation law in total Lagrangian description is expressed in current configuration as

$$\frac{1}{\det \mathbf{F}} \frac{\partial \bar{C}}{\partial \tau} + \frac{\partial}{\partial x} \left(\frac{F_{iK} \bar{J}_K}{\det \mathbf{F}} \right) \backslash * \text{MERGEFORMAT}$$

(S6)

by comparing equation (S5) for heat transfer and equation (S7) for mass diffusion, an analogy between them can be established by the following equivalence,

$$\begin{aligned} \bar{C} &= T, \\ \tau &= t, \\ \frac{F_{iK} \bar{J}_K}{\det \mathbf{F}} &= f_i, \quad \backslash * \text{MERGEFORMAT (S7)} \\ \frac{1}{\det \mathbf{F}} &= \rho \frac{dU}{dT}, \\ r &= 0 \end{aligned}$$

the deformation gradient \mathbf{F} is extracted from ABAQUS subroutine UMAT and the above specifically defined heat transfer behavior is implemented using UMATHT.

Furthermore, the compositional (equivalence thermal) expansion for large deformation is given by

$$\varepsilon^{(N)} = \frac{\beta(T^{(N)} - T^{(N-1)})}{1 + \beta T^{(N-1)}} \backslash * \text{MERGEFORMAT(S8)}$$

which is implemented using subroutine UEXPEN, and the deformation

dependent flux for the current state is given by Nanson's formula

$$\bar{j} = \frac{\bar{J}}{\det \mathbf{F} \sqrt{(N_K F_{Ki}^{-1})(N_L F_{Li}^{-1})}} \quad \backslash * \text{ MERGEFORMAT}$$

(S9)

which is implemented using DFLUX.

As shown in figure S4, the thickness of silicon film and Cu current collector in FEA is $H=300\text{nm}$. The length of the model is $L=5H=1500\text{nm}$. Bottom of Cu is fixed, and the displacement on y direction is zero on the left and right side. FEA mesh on the half of the model is also shown in figure S4. The elastic module of Cu is $E=120\text{GPa}$, the Poisson ratio $\nu=0.3$. The mechanical and electrochemical parameters of silicon are given in table S1. For silicon, a classical bilinear elastic-plastic mode was used, and the elastic module is linearly depended on the concentration of lithium $E=130-40\text{GPa}$ for $c=0-1$.

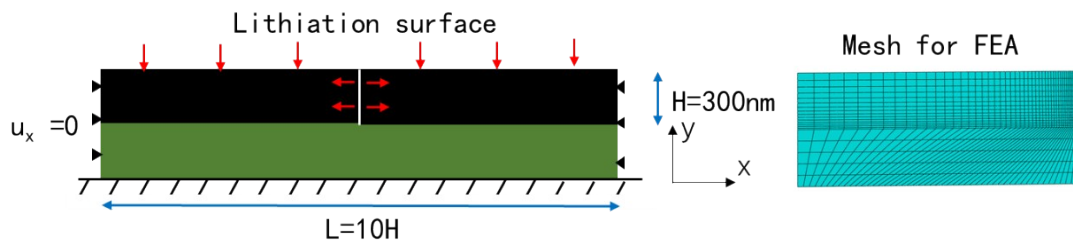


Figure S4. geometric model for finite element analysis (FEA).

Table S1. Parameters of silicon used in simulation

| Parameter | | Unit | Value |
|--------------------|------------|------|--------|
| Elasticity Modulus | $E(c)$ | GPa | 130-40 |
| Yield Stress | σ_Y | GPa | 0.26 |
| Plastic Modulus | E_p | GPa | 1.83 |

| | | | |
|--------------------------|-----------|-------------------------------------|-------------------|
| Poisson ratio | ν | -- | 0.3 |
| Expansion Coefficient | β | -- | 0.4 |
| Maximum Li concentration | C_{max} | mole m ⁻³ | 0.3667e6 |
| Diffusivity | D_0 | m ² /s | 10 ⁻¹² |
| Gas constant | R | JK ⁻¹ mole ⁻¹ | 8.314 |
| Room temperature | T | K | 300 |

3 Finite element analysis (FEA) for the lithiation in the first cycle.

The stress states during the first discharge progress were shown in Fig. S5. At the interface, the normal stress σ_{yy} and the shear stress σ_{xy} are very small.

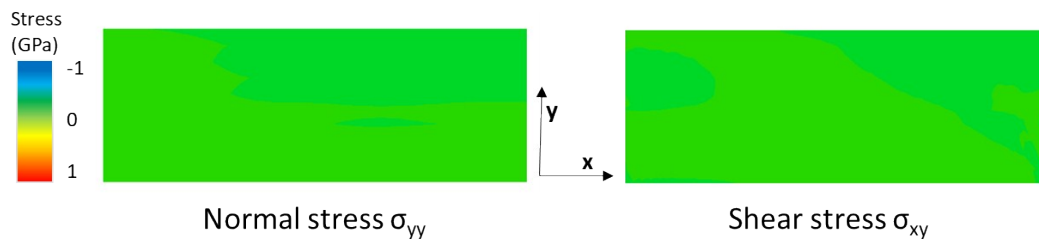


Figure S5. The stress states during the first discharge progress.